Biomolecules and Biomedicine ISSN: 2831-0896 (Print) | ISSN: 2831-090X (Online) Journal Impact Factor® (2024): 2.2

www.biomolbiomed.com | blog.bjbms.org

The BiomolBiomed publishes an "Advanced Online" manuscript format as a free service to authors in order to expedite the dissemination of scientific findings to the research community as soon as possible after acceptance following peer review and corresponding modification (where appropriate). An "Advanced Online" manuscript is published online prior to copyediting, formatting for publication and author proofreading, but is nonetheless fully citable through its Digital Object Identifier (doi®). Nevertheless, this "Advanced Online" version is NOT the final version of the manuscript. When the final version of this paper is published within a definitive issue of the journal with copyediting, full pagination, etc., the new final version will be accessible through the same doi and this "Advanced Online" version of the paper will disappear.

RESEARCH ARTICLE

Zhou et al: MSC EVs reprogram macrophages in sepsis

Adipose-derived MSC extracellular vesicles ameliorate sepsis by reprogramming macrophages via miR-21-5p targeting PELI1

Guannan Zhou^{1,2#}, Jieqiong Song^{1#}, Lizhen Xuan¹, Zhunyong Gu¹, Yimei Liu¹, Cheng Xu^{3#*}, Hongyu He^{1#*}

¹Department of Intensive Care Unit, Zhongshan Hospital, Fudan University, Shanghai, China;

²Department of Gynecology, The Obstetrics and Gynecology Hospital of Fudan University, Shanghai, China;

³Department of Breast Surgery, Yangpu Hospital, School of Medicine, Tongji University, Shanghai, China.

#Equally contributed to this work: Guannan Zhou, Jieqiong Song, Cheng Xu, and Hongyu He.

*Correspondence to Hongyu He: <u>he.hongyu@zs-hospital.sh.cn</u> and Cheng Xu: xucheng@live.cn.

DOI: https://doi.org/10.17305/bb.2025.11971

ABSTRACT

Sepsis is a common and life-threatening condition encountered in intensive care units (ICUs). Mesenchymal stromal cells (MSCs) and their small extracellular vesicles (EVs) have emerged as promising nanotherapeutics, particularly in the context of COVID-19. This study evaluates the efficacy and mechanisms of adipose-derived MSC EVs (ADMSC-EVs) in a lipopolysaccharide (LPS)-induced sepsis model. We quantified M2 macrophages and IL-10 in peripheral blood mononuclear cells (PBMCs) from both septic patients and healthy donors. ADMSCs and their EVs were isolated, and EVs were administered to LPS-challenged mice. Macrophage phenotypes in lung tissue were analyzed using flow cytometry and immunofluorescence. The biodistribution of EVs was traced with PKH67 green fluorescent cell linker dye (PKH-67), and the signaling pathways involved in macrophage reprogramming were examined. ADMSC-EVs efficiently entered macrophages, promoted M2 polarization, suppressed inflammation, and improved survival rates in septic mice. Biodistribution studies demonstrated widespread organ accumulation, with notable localization in the lungs, liver, and kidneys. Mechanistically, the EV cargo miR-21-5p targeted Pellino E3 ubiquitin protein ligase 1 (PELII), driving M2 polarization in vivo, which was accompanied by increased IL-10 levels. These findings position ADMSC-EVs as a viable cell-free therapeutic approach for mitigating LPS-induced sepsis through the delivery of miR-21-5p to PELII, thereby supporting further development of EV-based immunomodulatory strategies for sepsis management.

Keywords: ADMSCs, extracellular vesicles, EVs, sepsis, macrophages, IL-10, miR-21-5p.

INTRODUCTION

Sepsis represents a systemic infection syndrome that triggers immune dysregulation and can lead to multiple organ dysfunction[1, 2]. Increasing evidence indicates that sepsis is a leading cause of mortality in intensive care units (ICUs) across the US and Europe[3, 4]. The pathophysiology of sepsis involves a complex interplay among the immune system, the microbiome, and host tissues. Consequently, regulating the inflammatory response remains a major challenge in sepsis management. Although inflammation is essential for controlling infection, excessive or prolonged activation can lead to tissue damage, organ dysfunction, and ultimately, sepsis-induced death. The current standard treatment for sepsis involves antibiotics, fluid resuscitation, corticosteroids, and vasopressors, but these therapies primarily focus on symptom management and infection control rather than correcting the underlying immune dysfunction. Early and broad-spectrum antibiotic therapy is the cornerstone of sepsis treatment, aiming to target the underlying infection. However, the emergence of antimicrobial resistance has become a significant challenge in treating sepsis effectively[5, 6]. Corticosteroids are sometimes used to counteract the inflammatory response in severe sepsis. However, the use of corticosteroids remains controversial, as they can suppress the immune system, increase the risk of secondary infections, and prolong ICU stays[7]. New approaches including addressing immune modulation and regulating tissue repair are acknowledged as promising strategies. Therapeutics to restore macrophage function, promote immune tolerance, and modulate the inflammatory response could be a potentially valuable adjunct to existing therapies in sepsis management.

Mesenchymal stem cells (MSCs) possess potent immunomodulatory effects that contribute to reducing sepsis severity. MSCs, which are multipotent stromal cells capable of differentiating into various cell types, can modulate immune responses, promote tissue regeneration, and accelerate healing processes. Mechanistically, MSCs could reduce pro-inflammatory cytokines meanwhile simultaneously increasing

anti-inflammatory cytokines[8-10]. Recently, adipose-derived MSCs (ADMSCs) have emerged as promising candidates for potential clinical application. Researchers has demonstrated that ADMSCs could alleviate liver injury[11], reduce the systematic inflammation[12], promote tissue regeneration, and enhance survival outcomes in septic models.

Extracellular vesicles (EVs), as nanocarriers derived from diverse cell types, facilitate intercellular communication by delivering bioactive cargo to recipient cells[13-16]. One of the key mechanisms by which ADMSCs exert their therapeutic effects is through the secretion of EVs, which are nanosized membrane-bound particles that carry a variety of bioactive molecules, including proteins[17], lipids, and RNA[18, 19]. EVs derived from adipose-derived mesenchymal stem cells (ADMSCs) exhibit anti-inflammatory, immunomodulatory, and regenerative properties, making them promising candidates for sepsis therapy. Among their bioactive cargos, microRNAs (miRNAs) have emerged as key regulators of gene expression. These small, non-coding RNAs are involved in fine-tuning cellular responses and can influence a biological processes, including wide of immune regulation[20], inflammation[21], and tissue repair. miRNAs packaged within ADMSC-derived EVs have been found to play a key role in modulating macrophage polarization and function, which is critical in the context of sepsis. Increasing studies indicated that miR-21-5p could inhibit LPS-induced inflammatory injuries [22, 23], meanwhile the decrease of exosomal miR-21-5p is associated with the development of sepsis in polytraumatized patients[24]. Another study showed that endothelial progenitor cells-derived exosomal microRNA-21-5p alleviates sepsis-induced acute kidney injury by inhibiting RUNX1 expression[25]. In addition, our previous study revealed that high levels of miR-21-5p are present in MSCs and MSC-derived EVs[13]. Therefore, understanding the role of ADMSC-derived EV miRNAs in sepsis treatment is crucial for developing effective cell-free therapeutic strategies that harness the power of stem cell-derived vesicles. This led us to hypothesize that ADMSC-EVs containing specific miRNAs could similarly alleviate related disorders. Here, we investigate the role of ADMSCs-EVs enriched with miR-21-5p in sepsis suppression and delineate the underlying mechanisms involved. Understanding the molecular mechanisms underlying EVs-mediated effects in sepsis could pave the way for new, more targeted treatments for this devastating condition.

MATERIALS AND METHODS

Ethics statement

This study was conducted according to the approval from the Ethical Committee of Zhongshan Hospital, Fudan University, the approve number is B2022-107R (2022-03), with informed consent obtained from all patients. All personal data collected during the study will be anonymised before analysis, ensuring that no identifiable information is retained. In addition, any biological samples provided may be stored in a certified biobank for future ethically approved research. All animal procedures were performed in accordance with the protocol approved by the Institutional Animal Care and Use Committee at the Fudan University (SYXK2020-0032).

Clinical samples

Patients with sepsis (n=10) and non-sepsis donors (n=10) were enrolled to collect fresh peripheral blood samples at Zhongshan Hospital, Fudan University from 2020 to 2023, with no significant differences between the sepsis and non-sepsis donor groups regarding demographic characteristics, including age, sex, ethnicity, underlying disease conditions, and infection types. Separation of peripheral blood mononuclear cells (PBMCs) was performed by EasySep kit (STEMCELL Technologies, Canada).

Isolation of peripheral blood mononuclear cells (PBMCs) and analysis

The PBMCs were collected from the septic patients and non-sepsis donors. Normally, we collect 10 mL of peripheral blood in collection tubes (containing EDTA anticoagulant) and finish the isolation within 2 hours. Add 10 mL PBS into 10 mL

peripheral blood in 50 mL falcon tube, and add them on 20mL Lymphoprep (# 07861, STEMCELL Technologies, Canada) solution in a new 50 mL falcon tube. Centrifuge the tubes at 600 g for 20 min. Collect the PBMCs layer (white layer in the middle) into a new 50 mL falcon tube, wash twice by PBS. Then, culture the PBMCs in RPMI-1640 (containing 10% FBS and 1% penicillin and streptomycin) or freeze the PBMCs in -80°C.

For qPCR, total RNA was isolated and purified using RNApure extraction kit (BioTeke Corporation, Beijing, China) according to the manufacturer's instructions. Afterward, the cell lysates using Trizol reagent (Invitrogen, United States) were extracted to determine the mRNA level.

For cytometry, cells were first incubated with 2% FBS in PBS to block non-specific binding sites, followed by the surface staining with fluorochrome-conjugated antibodies against specific markers for 30 minutes at 4°C in the dark. Then, we conducted the intracellular staining for IL-10 and IL-6. Then, cells were fixed and permeabilized using Fixation/Permeabilization solution (BD Biosciences) and then stained with the corresponding intracellular antibodies. Samples were analyzed using a CytoFLEX S Flow Cytometer (Beckman Coulter).

ADMSCs production

The ADMSCs were collected from the mice to produce the ADMSCs-EVs. Normally, we used six C57BL/6 mice (including 3 male mice and 3 female mice) for each ADMSCs production batch. These mice are all 6 weeks old mice. All the animals were randomly assigned to groups, and the randomization process was conducted to ensure unbiased allocation of subjects. Firstly, we collected the adipose tissue samples from the inguinal fat pad of C57BL/6 mice. Then we cut the adipose tissues into small pieces, followed by the digestion by using 0.1% type I collagenase solution (Gibco, Grand Island, NY, USA) for 30 minutes. Then we used 10 mL DMEM (containing 20% FBS) to stop the digestion. After the filtration through 70 µm nylon mesh for twice, the suspension was centrifuged at 1500 g for 5 min to isolate the cells. The

cells were resuspended and incubated in DMEM (containing 10% FBS plus 100 U/mL penicillin and streptomycin). We mixed all these cells and cultured them together in DMEM (containing 10% FBS plus 100 U/mL penicillin and streptomycin).

Isolation and purification of ADMSCs-EVs

Firstly, we prepared the EVs-free FBS for cells culture. The FBS was centrifuged for 12 hours at 120,000 g to remove the EVs. Secondly, we cultured the isolated ADMSCs by using EVs-free FBS DMEM medium. The conditioned medium (after cell culture) was collected to centrifuge as below: for 30 min at 2000 g to remove cell debris or apoptotic bodies, followed by the tangential flow filtration (TFF), as reported in many previous studies[26-29]. The ADMSC-EVs were re-suspended by cold PBS, followed by the filtration with 0.22 µm filter. The characterization assays include transmission electron microscopy (TEM), nanoparticle size analysis (NTA) and western blot. In the TEM assay, the diluted EVs were loaded into the carbon-coated copper electron microscope grids for 1 min and negatively stained with phosphotungstic acid for 10 min. The images were observed under TEM (FEI Tecnai G2 Spirit Twin, Philips, NL). In the NTA assay, EVs were dissolved in 1000 uL PBS. Then, the particle size distribution of EVs was directly demonstrated in the NanoSight nanoparticle tracking analyzer (NTA; Malvern, UK).

Plasmids production and plasmids transfection

The Plex-CD63 (Addgene, #168220) and Plex-GFP (Addgene, #162032) was acquired from Addgene. The "Plex-CD63-GFP" plasmid was cloned through the purchased plasmids by using restriction enzymes.

Cells were seeded in the flask 12 hours prior to the transfection. ADMSCs were seeded in T225 flasks with 30 mL culture medium, at 37°C and 5% CO2. For one T225 flask, Plasmid (25 µg) was mixed with 3mL Opti-MEM (Thermo Fisher Scientific) for 5 minutes, meanwhile PEI⁴⁰⁰⁰ (40816ES02, Yeasen Biotechnology) (50

 μ L for 1 μ g/ μ L) for was mixed withOpti-MEM (Thermo Fisher Scientific) for 5 minutes. Then mix the two solutions for 20 minutes, followed by adding them into the flasks. For EVs production, medium was changed as EVs-free DMEM (containing 10% EVs-free FBS) for 48 hours. The tangential flow filtration (TFF) was used to purify the EVs to get rid of the residual plasmids and PEI. The supernatant was collected to isolate the EVs.

Enzyme-linked immunosorbent assay (ELISA)

THP-1 cells incubated in 24-well plates were treated with PMA to induce the M0 phenotype. Then, PBS (C0221A, Beyotime Biotechnology), THP1-EVs and ADMSCs-EVs were added to treat the M0 cells for 48h. Human IL-6 ELISA kit (ab178013) and human IL-10 ELISA kit (ab185986) were used to measure the expression of counterpart according to the manufacturer's specifications. In the animal assay, plasma was analyzed using ELISA kits (ab222503) and mouse TNF alpha ELISA Kit (ab208348) according to the manufacturer's specifications.

Immunofluorescence and confocal microscopy

For ADMSCs characterization, immunofluorescence assays were performed. The cells on round coverslips were fixed in 4% paraformaldehyde for 20 min and permeabilized with 0.3% Triton X-100 for 20 min. Cells were blocked the with blocking buffer (Solarbio). Primary antibody and secondary antibody were diluted in Immunofluorescent Staining Dilution Buffer (Beyotime Biotechnology). The cells were incubated the cells with primary antibodies and second antibodies following the manufacturer's specifications. Anti-CD90 (ab307736), Anti-CD105 (ab221675) and Alexa Fluor 488 Goat anti-Rabbit secondary antibody (A0423, Beyotime Biotechnology) were used. Images were captured via a confocal microscope (Nikon, Japan).

EV labelling

The EVs were labelled by PKH67 (Sigma-Aldrich PKH67GL) according to the manufacturer's instructions and previous studies[30, 31]. Briefly, EVs in PBS were added to 0.5 mL of Diluent C, and 3 μ L of PKH67 was added to 0.5 ml of Diluent C; the two reaction mixtures were incubated at room temperature for 20 minutes. Then 20 mL of EVs-free FBS was added to prevent the excessive labelling, followed by the ultracentrifugation at 125,000 \times g for 1 hour to remove the residual dye. The recipient cells were treated with the PKH67-labelled EVs for 4 hours. Then the cells were washed with PBS twice and fixed with 4% paraformaldehyde (PFA) for 10 min, followed by the staining with mCherry-Actin-Tracker and DAPI, respectively. The samples were observed and captured via a confocal microscope (Nikon, Japan).

Animal assay

Normally, we used six C57 mice (including 3 male mice and 3 female mice) for each ADMSCs production batch. These mice are all 6 weeks old mice for the LPS-mediated sepsis model. We grouped the LPS-mediated sepsis mice into three groups randomly (N =5 mice/group: 2 male and 3 female) as below: LPS group (subjected to LPS treatment only), LPS+PBS group (subjected to LPS followed by PBS intravenous injection), ADMSCs-EVs group (subjected to LPS followed by ADMSC-EVs (PKH-67 labeled) intravenous injection). All the animals were randomly assigned to groups, and the randomization process was conducted to ensure unbiased allocation of subjects. Mice were put into the induction box after filling it with isoflurane (2.5% induction concentration) for about 40 seconds. Then, the induction box was closed, and the mouse was completely anesthetized (this process takes about 1.5 min). The induction box can be gently shaken to check whether the mouse is fully anesthetized. If the mouse is fully anesthetized, its body will be overturned into a side position and not restored from the lying position. Briefly, 4 mg/kg of LPS was administered intraperitoneally to induce sepsis. Then, 10¹¹ particles of ADMSC-EVs were injected intravenously at 0, 6, and 12 hours. As a control, an equivalent volume of PBS was injected in the same manner. We assessed the animals every 6 hours during the initial 48 hours after the procedure and then every 12 hours for 6 days. At last, all mice were euthanasia via intraperitoneal injection of pentobarbital sodium at a dosage of 150 mg/kg and sacrificed. The animal experiments were conducted following the guide for the care and use of laboratory animals (SYXK2020-0032). We were unaware of group assignments during the study for blinding to reduce bias. Euthanasia was performed when animals showed signs of weight loss exceeding 20%. All euthanasia procedures were conducted in accordance with institutional ethical guidelines and following veterinary oversight to minimize animal suffering.

Phenotyping THP-1 cells

THP-1 is a human leukemia monocytic cell line, which has been widely used to study monocyte/macrophage functions[32, 33]. The cells were treated with 100 nM phorbol 12-myristate 13-acetate (PMA, Sigma-Aldrich) for 24 hours. To induce M2 macrophage polarization, replace the differentiation medium with RPMI-1640 supplemented with 10% FBS and the following polarization agents: IL-4 (20 ng/mL) and IL-13 (20 ng/mL), which are key cytokines known to drive M2 polarization. Both cytokines activate the STAT6 pathway, promoting the anti-inflammatory M2 phenotype. Then the induced cells were detected by flowcytometry assay.

Flow cytometry

We cultured the ADMSCs and tested the expression of surface biomarkers at the 3rd passage. The FITC-CD90 (ab25672), FITC-CD105 (ab314950) antibodies were used to phenotype the ADMSCs by flowcytometry. As for the *in vivo* assay, half of the lung tissues were used for immunofluorescence assay, and another half part was lysated as single cell suspension for flow cytometry. PE-Cy7 Mouse Anti-Human CD68 (BD Pharmingen, 565595), FITC Mouse Anti-Human CD206 (BD Pharmingen, 551135) and FITC Rat Anti-Mouse IL-10 (BD Pharmingen, 554466) were used for staining the

macrophages. The THP-1 phenotyping assay, the induced cells were stained by the CD68, CD206 antibodies. In the flowcytometry assay to evaluate the role of ADMSC-EVs^{GFP} in septic mice, antibodies of PE Rat Anti-Mouse F4/80 (BD Pharmingen, T45-2342), Alexa Fluor 647 Rat Anti-Mouse CD206(BD Pharmingen, MR5D3) were selected. All the incubations for primary conjugated antibodies were conducted in room temperature.

Western blot assay

Total protein was extracted using RIPA buffer (P0013C, Beyotime Biotechnology) containing 1 mM phenylmethylsulfonyl fluoride (PMSF). Protein concentrations were determined by the Bradford protein quantity assay kit. A total of 20 μg of EVs or cell lysates were resuspended in 5 × SDS loading buffer, subsequently incubated at 100°C for 20 min. Then, the supernatant was separated by 10% SDS-polyacrylamide gel (Beyotime Biotechnology) and transferred to PVDF membranes (Millipore), which were blocked with blocking buffer (Beyotime Biotechnology) for 1 h, incubated with the primary antibodies at 4°C overnight, and then incubated with secondary antibodies at for 1 h. An ECL kit (Beyotime Biotechnology) was used to detect the bands. The EVs were detected by anti-CD63 (ab134045), anti-Alix (ab275377) and anti-Tsg101 (ab133586), which was well acknowledged in previous studies[34-37]. The cell samples were detected by anti-IL10 (ab52909) and anti-Tubulin (ab6160).

Quantitative Real-Time PCR

For EV miRNAs measurement, the RNA extraction was conducted from isolated extracellular

vesicles by an miRNeasy Micro Kit (Qiagen).

Gene expression of *CD163*, *Arg1* and *IL-10* at mRNA level were detected. Briefly, total RNA was isolated and purified using RNApure extraction kit (BioTeke Corporation, Beijing, China) according to the manufacturer's instructions. Cells treated with PBS were used as the controls. Afterward, the cell lysates using Trizol

reagent (Invitrogen, United States) were extracted to determine the mRNA level of CD163, Arg1 and IL-10. The real-time PCR (RT-PCR) experiment was performed using the TB Green premix Ex Taq II (TaKaRa Biotechnology, Dalian, China) in CFX96 Real-Time PCR Detection System (Bio-Rad, United States). The levels of miR21-5p were normalized against U6 snRNA (MQP-0202, RiboBio, Guangzhou, China) and we calculated the result with the $2^{-\Delta\Delta CT}$ method. The relative expressions of genes were calculated using the $2^{-\Delta\Delta CT}$ method with GAPDH as an internal reference. The specific primers were listed as below in Table 1.

Luciferase Reporter Assays

First, the potential targets of miR-21-5p were predicted using TargetScan (http://www.targetscan.org) and miRanda (http://miranda.org). The fragments of the PELI1 3' UTR containing either the wild-type (WT) or mutant (Mut) predicted miR-21-5p binding site were then subcloned into the pmirGLO vector (RiboBio). Subsequently, cells were cultured and seeded in 24-well plates for further analysis. Briefly, miR-21-5p mimics (miR-21-5p mimic: 5'-CAACACCAGUCGAUGGGCUGU-3') or control (NC) (Control (NC): 5'-UUCUCCGAACGUGUCACGUTT-3') sequences (RiboBio) co-transfected with pmirGLO-PELI1 WT or pmirGLO-PELI1 Mut constructs. MiR-21-5p mimic (B02003), mimic control (MC, B04002), inhibitor (B03001) and inhibitor control (B04003) were synthesized by Genepharma (Shanghai, China). After 48 hours of transfection, cells were harvested and lysed. Firefly luciferase and Renilla luciferase substrates were then added, and luciferase activity was measured using the Dual-Glo Luciferase Reporter Assay System (Promega). The luciferase assay results were analyzed following the manufacturer's instructions.

Ethical approval

This study was conducted according to the approval from the Ethical Committee of Zhongshan Hospital, Fudan University, the approve number is B2022-107R (2022-03),

with informed consent obtained from all patients. All animal procedures were performed in accordance with the protocol approved by the Institutional Animal Care and Use Committee at the Fudan University (SYXK2020-0032). The study was performed in accordance with the ethical standards as laid down in the <u>Declaration of Helsinki</u>.

Statistical analysis

Values in this study are presented as mean \pm SEM. We determined the statistical differences by using the unpaired two-tailed Student's t test or Mann-Whitney test, as appropriate. Kaplan-Meier survival plots and log-rank tests were used to compare survival results among treatment groups. *p < 0.05, **p < 0.01, and ***p < 0.001. Statistical significance was defined as p < 0.05.

RESULTS

3.1 Altered M2 Macrophage Proportion and IL-10 Expression in Peripheral Blood of Sepsis Patients

To explore the potential roles of macrophages in sepsis, we analyzed the CD68+CD206+ macrophages (M2) subpopulation in septic patients' peripheral blood mononuclear cell (PBMC) (Figure 1A). As depicted in Figure 1B and Figure 1C, the results revealed a significantly reduced proportion of CD68+CD206+ M2 macrophages in septic patients than those without sepsis. Additionally, the mRNA expression level of *Arg1*, *CD163* and *CD68* in PBMCs from septic patients were lower than those in non-septic patients. Furthermore, the cytokine expression level of IL-10 in serum from septic patients decreased, while the IL-6 level was elevated. Collectively, these findings suggest that the M2 macrophage and IL-10 expression are diminished in sepsis, indicating their critical role in mitigating the progression of sepsis.

Characterization of ADMSCs and ADMSCs-EVs and their potential in sepsis therapy

We aimed to assess the therapeutic potential of ADMSCs and ADMSCs-EVs in mitigating sepsis. We performed a comprehensive identification process involving the adherence ability, surface marker expression, and differentiation potential. As demonstrated in Figure 2A, results indicated that ADMSCs exhibit spindle-like morphology and adhere well. Meanwhile, the immunofluorescence results (Figure 2B and 2C) and flow cytometry results (Figure 2D and 2E) confirmed the expression of surface markers CD105 and CD90, consistent with established published MSCs characteristics. As for the EVs isolation and characterization, ADMSCs-EVs were isolated by using the tangential flow filtration (TFF), as reported in many previous studies[26]. And we conducted the characterization of ADMSCs-EVs by using Nanoparticle Tracking Analysis (NTA) and Transmission Electron Microscope (TEM). We found that the ADMSCs-EVs were identified as cup-shaped structures (Figure 2H) with diameters predominantly ranging from 30 to 500 nm (Figure 2F). In addition, marker proteins such as CD63, Alix, and Tsg101 were detected on the ADMSCs-EVs (Figure 2G, Supplementary Figure S1). The secretion efficiency of ADMSCs was analyzed by NTA (Supplementary Figure S2). Collectively, we isolated ADMSCs and subsequently collected ADMSCs-EVs.

ADMSC-EVs induce M2 polarization in vitro

We evaluated the uptake of ADMSC-EVs and their role in macrophages reprogramming and polarization. As results from Supplementary Figure S3, we treated the THP-1 cells for 72h. The PKH-67 labeled ADMSCs-EVs were shown to enter the mCherry-Actin Tracker labeled THP-1 (phenotyping as Supplementary Figure S4) cells (nucleus were labeled by DAPI) effectively (Figure 3A). As depicted in Figure 3B and Figure 3C (Supplementary Figure S5), THP-1 cells treated with ADMSC-EVs exhibited significantly higher levels of CD206 expression than treated with PBS or THP-1-EVs. Similar results were obtained with primary mouse

monocytes that ADMSC-EVs led to a higher percentage of the F4/80+CD206+ macrophage subpopulation than PBS or monocytes-EVs (Figure 3D and 3E, Supplementary Figure S6). Additionally, ADMSC-EVs significantly increased the mRNA expression level of *CD163*, *Arg1* and *IL-10* in both THP-1 cells (Figure 3F) and primary monocytes (Figure 3G) compared to controls. Furthermore, the protein expression level of IL-10 in ADMSC-EVs treated monocytes is higher in PBS group and monocytes-EVs group (Figure 3H, Supplementary Figure S7, Supplementary Figure S11). These results collectively indicate that ADMSC-EVs effectively promote macrophages (both THP-1 cells line and primary mouse monocytes) polarization.

ADMSC-EVs mitigate LPS-mediated sepsis by inducing macrophages polarization in mice

To evaluate the protective effects of ADMSC-EVs against endotoxic shock in LPS-induced sepsis model, mice received LPS followed by ADMSC-EV treatment (Figure 4A). As depicted in Figure 4B and Figure 4C, IL-6 and TNF-α level in ADMSC-EVs treated LPS-induced septic mice were significantly lower than in control groups. Notably, mortality rates were substantially reduced in the ADMSC-EV group compared to control groups (80% mortality due to the LPS-induced sepsis). Flow cytometry analyses revealed an increased percentage of F4/80+CD206+ macrophages and F4/80+CD206+IL-10+ macrophages in ADMSC-EVs treated LPS-mediated septic mice (Figure 4E and Figure 4F).

ADMSC-EVs reduce the inflammatory by increasing IL-10 expression in M2 macrophages *in vivo*

To investigate the influence of ADMSC-EVs on IL-10 secretion from M2 macrophages, we analyzed the macrophage uptake M2 phenotype *in vivo*. We firstly isolated the macrophages from the mice lung and then detected the percentage of M2 phenotype macrophage. As depicted in Figure 5A and Figure 5B, ADMSC-EVs treatment increased the percentage of M2 macrophages in the lung compared to

controls. Additionally, confocal microscopy demonstrated that F4/80 positive macrophages in the lung were able to uptake PKH-67 labeled ADMSC-EVs (Figure 5C). Furthermore, flow cytometry and immunofluorescence results confirmed that ADMSC-EVs treatment elevated IL-10 levels in pulmonary macrophages (Figure 5C and 5D), suggesting a mechanism for reducing pulmonary inflammation through enhanced M2 polarization and IL-10 secretion. Also, we tested the pathological changes in mice treated with LPS or ADMSC-EVs by HE staining, which shows the ADMSC-EVs exhibited ability to ameliorates sepsis in Lung (Supplementary Figure S8). We also added the effect of ADMSC-EVs on different immune cell populations, such as T cells, neutrophils, and dendritic cells, which showed that the ADMSC-EVs could increase the expression of CCR7 in DC cells, decrease the CCR2 expression in neutrophils (Supplementary Figure S9).

Biodistribution of ADMSC-EVs in LPS-induced septic mice

We further assessed the biodistribution of ADMSC-EVs in LPS-induced sepsis. A plasmid expressing the fused protein CD63-GFP (Figure 6A) was transfected into ADMSCs to track EVs *in vivo* (Figure 6B). As depicted in Figure 6C, ADMSC-EVs^{GFP} were injected into the LPS-induced septic mice to evaluate the biodistribution of the ADMSC-EVs^{GFP} in mice. As demonstrated in the Figure 6D, the ADMSC-EVs^{GFP} could enter and be encapsulated in the lungs, liver, and kidneys of septic mice (Figure 6E). Furthermore, a significant proportion of M2 macrophages in these organs were GFP positive, indicating the successful induction and reprogramming by ADMSC-EVs. Collectively, the ADMSC-EVs could enter the liver, lung and kidney, and play vital roles in macrophages polarization.

ADMSCs-EVs encapsulated miR-21-5p targets PELI1 in macrophages

It was widely reported that decreased *PELI1* expression in macrophages is associated with inhibition of inflammation[38]. In the current study, the results indicated that the expression level of *PELI1* in PBMCs from sepsis patients is higher than the

expression level of *PELI1* in PBMCs from normal patients (Figure 7B). Meanwhile, the expression of miR-21-5p in ADMSCs-EVs is higher than in THP-1 EVs (Figure 7A). Mechanistically, we conducted the analysis upon the potential target predictive genes of miR-21-5p by using TargetScan. As demonstrated in Figure 7D, *PELI1* was predicted to be a target gene of miR-21-5p. Additionally, dual-luciferase assays confirmed that miR-21-5p binding to *PELI1* resulted in decreased luciferase activity (Figure 7C). Additionally, upregulation of miR-21-5p led to reduced PELI1 level and MAPK level in THP-1 cells (Figure 7E and Figure 7F, Supplementary Figure S8, Supplementary Figure S11). These findings indicate that ADMSCs-EVs encapsulated miR-21-5p can target PELI1 in macrophages, promoting M2 macrophages polarization during sepsis.

DISCUSSION

Sepsis is recognized as a syndrome of organ dysfunction caused by the dysregulation of host's response to systemic infection. It remains one of the most challenging and life-threatening conditions in modern medicine, with no effective treatment currently available beyond supportive care. As a leading cause of death in critically ill patients, sepsis represents a significant global healthcare challenge[39, 40]. Increasing evidence suggests that sepsis triggers a robust innate immune response, primarily mediated by macrophages. Macrophages are heterogeneous immune cells with diverse functions and are broadly categorized into classically activated M1 macrophages and alternative M2 macrophages, which exhibit pro-inflammatory and anti-inflammatory properties, respectively[41, 42]. M1-Macrophages are primarily involved in pro-inflammatory processes, and hyperactivated M1-Macrophages are a major source of pro-inflammatory cytokines, such as IL-6 and TNF- α , which contribute to tissue damage during infections[43]. In contrast, M2-Macrophages play crucial roles in tissue repair and resolution of inflammatory[44]. For example, studies have shown that M2-Macrophages transplantation can reduce the production of

proinflammatory cytokines (e.g., IL-6 and TNF- α) in animal models of acute kidney injury and colitis[45, 46].

Stem cells have garnered significant interest for clinical applications due to their differentiation potential [47]. Adipose tissue derived MSCs (ADMSCs) have also emerged as a promising alternative for cell-based therapy, offering advantages such as ease of access, ethical acceptance, and abundant availability [48, 49]. ADMSC-based therapies have shown the potential to modulate inflammation, promote tissue regeneration, and improve prognosis in various conditions [50, 51]. Consequently, we selected ADMSCs derived extracellular vesicles as nanocarriers for sepsis treatment. Most of the EVs in our study ranged from 30 to 200 nm, and a very small fraction of these particles larger than 200 nm. However, we defined these particles as EVs since it is difficult to sort the certain subpopulation in our study. It should be illuminated that the particles larger than 200 nm should be classed as micro-vesicles.

The immunofluorescence images in Figures 2B and 2C display cytoplasmic signals for CD105 and CD90. This is likely attributable to the permeabilization step applied during the staining procedure, which may have partially affected membrane integrity. However, the overall expression patterns are consistent with the expected surface marker profiles as confirmed by flow cytometry (Figure 2D and Figure 2E), which assesses surface marker expression without permeabilization.

Extracellular vesicles are nanosized particles (~30 to 1000nm) secreted by diverse types of cells[52, 53]. EVs retain bioactive properties similar to those of the donor cells, owing to the diverse biomolecules (e.g., proteins[54], nucleic acids[55], lipids, etc.) incorporated during the biogenesis process[56]. Furthermore, EVs retain their bioactivity even after prolonged storage and post-modification[57]. Our previous study demonstrated that the miR-21-5p is highly expressed in MSC derived EVs, and it has been reported that miR-21-5p plays a role in macrophages polarization[58, 59]. Therefore, it is logical to investigate the mechanisms of EVs (particularly those containing miR-21-5p) in influencing macrophages polarization. In addition, it is

indeed possible for murine-derived microRNAs (miRNAs) to regulate mRNA expression in human cells, despite the species difference. This regulatory effect is primarily based on the sequence complementarity and the conservation of target mRNA sequences across species. Our results are consistence to previous published studies[60, 61], which underscore the potential for murine miRNAs to regulate mRNA expression in human cells based on the conservation of miRNA-target interactions across species. Additionally, scaffold sorting proteins play a crucial role in EVs biogenesis. According to this mechanism, it is possible to engineer bioengineered EVs with diverse cargoes, including GFP proteins. Based on this approach, we generated the ADMSC-EVs^{GFP} to track the distribution of EVs in vivo. In the present study, we firstly evaluate the macrophages phenotypes in PBMC from septic patients and evaluate the IL-10 cytokine level in septic patients' serum. The results exhibited that the percentage of M2 macrophages is lower in septic patients' PBMC than non-septic patients' PBMC, while the IL-10 cytokine level in septic patients' serum is lower than non-septic patients' serum. These results are consistent with the results in other studies [62-65]. Then, we isolated the ADMSC and ADMSC-EVs, and characterized them by flowcytometry, TEM, NTA and western blot assays[10, 66]. We found that the ADMSC-EVs could enter the macrophages as recipient cells, which are in line with previous studies, and could induce the macrophages into M2 phenotype in vitro and ex vivo. These results are verified in flowcytometry assay, qPCR assay as well as western blot assay. Furthermore, in the animal experiment, we obtained the similar results that ADMSC-EVs could mitigate the LPS-induced sepsis and improve the prognosis by inducing the M2 polarization in vivo. In addition, by using the engineered EVs containing GFP to evaluate the distribution of ADMSC-EVs in the sepsis-induced mice, we engineered the plasmid named "CD63-GFP" to produce the ADMSC-EVsGFP, which is in line with previous study. According to the results from the flowcytometry assay, we found that the most of the M2 macrophages are GFP positive cells, which means that the cells

encapsulated the ADMSC-EVs are polarized into M2 phenotype. This intricate method could provide the evidence to support that the role of ADMSC-EVs in polarizing M2 macrophages *in vivo*, which could be widely applied in further studies. In this study, "F4/80+CD206+" represents mouse primary monocytes, while "CD68+CD206+" corresponds to human THP-1 derived macrophages. This distinction reflects the different marker profiles used for murine and human macrophages.

In vivo biodistribution studies of ADMSC-EVs were conducted to evaluate their tissue targeting profiles and to address concerns regarding potential off-target effects on non-immune cells. From the analysis of PBMCs, the ADMSC-EVs could increase the expression of CCR7 in DC cells, decrease the CCR2 expression in neutrophils. These results suggest that the potential therapeutic effect of ADMSC-EVs. Our findings indicate that while ADMSC-EVs could localize to lung, a large fraction is also detected in liver, suggesting the need for further optimization to enhance specificity and minimize unintended interactions.

PELI1 is a protein involved in regulating immune responses and inflammation[67]. It is a member of the PELI family of proteins, which are characterized by their peloton-like domains. PELI1 is particularly implicated in modulating the NF-κB signaling pathway, a central regulator of immune and inflammatory responses. Its functions are closely linked to the regulation of macrophage polarization, particularly the differentiation between pro-inflammatory (M1) and anti-inflammatory (M2) phenotypes. The downstream pathways of PELI1 inhibition in M2 macrophage polarization merit further investigation. It is crucial to explore whether other mediators or signaling pathways are involved in this process[68]. PELI1 (Pel-like 1) is a key regulator in immune responses, and its inhibition could potentially influence multiple signaling cascades that are central to macrophage polarization, particularly the NF-κB, JAK-STAT, and PI3K-AKT pathways. Additionally, cytokines such as IL-4, IL-13, and TGF-β, which are key drivers of M2 macrophage polarization, could be regulated through PELI1 inhibition. These cytokines activate various transcription

factors that promote M2 macrophage characteristics. The inhibition of PELI1 could potentially disrupt the signaling pathways initiated by these cytokines, leading to alterations in the polarization process.

Understanding how PELI1 interacts with these signaling pathways and mediators is essential for elucidating the broader molecular mechanisms underlying M2 macrophage polarization. This could also provide valuable insights into the therapeutic potential of targeting PELI1 in diseases where macrophage polarization plays a critical role, such as in chronic inflammation, tissue repair, and autoimmune diseases. We hypothesize that elevated PELI1 reflects upstream activation that drives the uncontrolled inflammation. That's why the higher PELI1 in septic PBMCs, and the therapeutics inhibit PELI1 expression could be helpful for mitigates inflammation. Regarding your concern about the use of PKH-67-labeled ADMSC-EVs in Figures 4 and 5 and ADMSC-EVs^{GFP} in Figure 6, we would like to clarify the rationale behind the different labeling strategies. PKH-67 is a lipid-soluble dye that is widely used for cell and vesicle tracking, but it may exhibit reduced fluorescence intensity over time due to potential dye dilution or degradation during in vivo circulation. To avoid this limitation, we used ADMSC-EVs^{^GFP} in Figure 6, which allows for more stable and reliable tracking of EVs, as GFP is a fluorescent protein that remains intact and stable in vivo. It is widely reported that CD63-GFP EVs is used to trace the EVs distribution[16, 69], the CD63 is scaffold protein of EVs, and does not influence the EVs distribution.

However, there are several limitations in the present study. First, a larger cohort of patients should be enrolled to further explore the relationship between M2 macrophages percentage and the severity of sepsis. Second, ADMSC-EVs should be tested in comparison with, or in combination with, current sepsis treatment to evaluate both the efficacy of single treatments and potential combination therapies. While some other additional controls, such as unlabeled ADMSC-EVs, PKH-67 dye alone, and control EVs (e.g., THP-1 EVs or miR-21-5p knockdown/overexpression variants)

are ideal for the result. We believe that our experimental design adequately addresses the primary research question without the need for these additional controls. Also, there should include seed-mismatch controls or rescue experiments, as well as EV-borne miR-21 entry and load-dependence experiments in the future studies. Specifically, our in vitro experiment results could verify that the relevant baseline controls in our experimental setup to ensure the LPS-induced sepsis model was appropriately validated. These controls are sufficient to assess the effects of ADMSC-EVs in the context of sepsis. Another concern is the mice number in survival assay, the decision to use n = 5 per group was based on preliminary data and considerations for resource availability. While small sample sizes are acknowledged as a limitation, this study was designed to explore preliminary trends and observe initial efficacy signals. We understand that smaller group sizes may introduce variability in survival data, particularly in high-lethality models, where a single survivor could disproportionately affect the interpretation of statistical significance. However, we believe this sample size provides valuable insights into the potential efficacy of the treatment under investigation. Furthermore, in our current study, we included a balanced mix of sexes $(2 \circlearrowleft / 3 \circlearrowleft per group)$, but we did not perform sex-stratified analyses due to the preliminary nature of the study and limitations in sample size. However, we understand the importance of exploring potential sex differences in the outcomes, and we plan to address this in future studies with larger sample sizes and more targeted analyses.

In this study, we explored the potential of ADMSC-derived extracellular vesicles (ADMSC-EVs) as a therapeutic approach for sepsis, focusing on their ability to modulate macrophage polarization and improve outcomes in sepsis. Our results indicate that in septic patients, there is a significant reduction in the proportion of M2 macrophages and a decrease in IL-10 cytokine levels in peripheral blood mononuclear cells (PBMCs) compared to non-septic controls. These findings highlight the disruption of the anti-inflammatory response in sepsis, which contributes to the

progression of the disease. We further demonstrated that ADMSC-EVs can effectively promote the polarization of macrophages to the M2 phenotype both in vitro and in vivo, as evidenced by flow cytometry, qPCR, and Western blot analysis. Importantly, the use of engineered ADMSC-EVs containing GFP enabled us to trace the distribution of these vesicles in vivo, confirming their ability to reach macrophages and induce M2 polarization in the LPS-induced sepsis mouse model. These results support the therapeutic potential of ADMSC-EVs in modulating the immune response in sepsis, particularly through the polarization of macrophages to the M2 phenotype, which is crucial for tissue repair and resolution of inflammation. Additionally, we investigated the role of PELI1 in regulating macrophage polarization and its potential as a target for therapeutic intervention. The inhibition of PELI1 appears to affect key signaling pathways, which are central to the polarization of macrophages, and could provide valuable insights into how ADMSC-EVs exert their effects. Despite the promising results, this study has limitations, including the need for a larger cohort of patients and further testing of ADMSC-EVs in combination with existing sepsis treatments. Nonetheless, our findings pave the way for future studies to optimize ADMSCs-EVs based therapies and explore their clinical applicability in sepsis and other inflammatory conditions.

CONCLUSION

In conclusion, our study demonstrates that ADMSC-EVs can reprogram macrophages into M2 phenotype and alleviate the LPS-mediated sepsis *in vivo*. Mechanistically, ADMSC-EVs deliver miR-21-5p to target PELI1, thereby promoting M2 macrophage polarization and enhancing IL-10 secretion. These findings provide promising insights into the therapeutic potential of ADMSC-EVs as a novel strategy for the treatment of sepsis.

Conflicts of interest: Authors declare no conflicts of interest.

Funding: Authors received no specific funding for this work.

Data availability: The datasets used and analyzed during the current study are available from the corresponding author on reasonable request.

Consent to participate: Freely given, informed consent to participate in the study was obtained from all participants (or their parent or legal guardian in the case of children under 16). The tissues were collected in Zhongshan Hospital (Shanghai, China) and Fudan University. No tissues were obtained from prisoners.

Submitted: January 2, 2025

Accepted: May 5, 2025

Published online: October 27, 2025

REFERENCES

- 1. Cecconi M, Evans L, Levy M, Rhodes A: Sepsis and septic shock. *Lancet* 2018, 392(10141):75-87.
- 2. Angus DC, van der Poll T: Severe sepsis and septic shock. *N Engl J Med* 2013, 369(9):840-851.
- 3. Seymour CW, Liu VX, Iwashyna TJ, Brunkhorst FM, Rea TD, Scherag A, Rubenfeld G, Kahn JM, Shankar-Hari M, Singer M *et al*: Assessment of Clinical Criteria for Sepsis: For the Third International Consensus Definitions for Sepsis and Septic Shock (Sepsis-3). *JAMA* 2016, 315(8):762-774.
- 4. Paugam-Burtz C, Levesque E, Louvet A, Thabut D, Amathieu R, Bureau C, Camus C, Chanques G, Faure S, Ferrandière M *et al*: Management of liver failure in general intensive care unit. *Anaesth Crit Care Pain Med* 2020, 39(1):143-161.
- 5. Legese MH, Asrat D, Swedberg G, Hasan B, Mekasha A, Getahun T, Worku M, Shimber ET, Getahun S, Ayalew T *et al*: Sepsis: emerging pathogens and antimicrobial resistance in Ethiopian referral hospitals. *Antimicrob Resist Infect Control* 2022, 11(1):83.
- 6. Chaurasia S, Sivanandan S, Agarwal R, Ellis S, Sharland M, Sankar MJ: Neonatal sepsis in South Asia: huge burden and spiralling antimicrobial resistance. *Bmj* 2019, 364:k5314.
- 7. Fang F, Zhang Y, Tang J, Lunsford LD, Li T, Tang R, He J, Xu P, Faramand A, Xu J *et al*: Association of Corticosteroid Treatment With Outcomes in Adult Patients With Sepsis: A Systematic Review and Meta-analysis. *JAMA Intern Med* 2019, 179(2):213-223.
- 8. Uccelli A, Moretta L Fau Pistoia V, Pistoia V: Mesenchymal stem cells in health and disease. *Nat Rev Immunol* 2008, 8(9):726-736.
- 9. Hu C, Li LA-OX: Preconditioning influences mesenchymal stem cell properties in vitro and in vivo. *J Cell Mol Med* 2018, 22(3):1428-1442.

- 10. Xia L, Zhang C, Lv N, Liang Z, Ma T, Cheng H, Xia Y, Shi L: AdMSC-derived exosomes alleviate acute lung injury via transferring mitochondrial component to improve homeostasis of alveolar macrophages. *Theranostics* 2022, 12(6):2928-2947.
- 11. Hu C, Zhao L, Li L: Current understanding of adipose-derived mesenchymal stem cell-based therapies in liver diseases. *Stem Cell Res Ther* 2019, 10(1):199.
- 12. Abreu SC, Antunes MA, Xisto DG, Cruz FF, Branco VC, Bandeira E, Zola Kitoko J, de Araújo AF, Dellatorre-Texeira L, Olsen PC *et al*: Bone Marrow, Adipose, and Lung Tissue-Derived Murine Mesenchymal Stromal Cells Release Different Mediators and Differentially Affect Airway and Lung Parenchyma in Experimental Asthma. *Stem Cells Transl Med* 2017, 6(6):1557-1567.
- 13. Zhu Z, Zhang Y, Zhang Y, Zhang H, Liu W, Zhang N, Zhang X, Zhou G, Wu L, Hua K *et al*: Exosomes derived from human umbilical cord mesenchymal stem cells accelerate growth of VK2 vaginal epithelial cells through MicroRNAs in vitro. *Hum Reprod* 2019, 34(2):248-260.
- 14. Zhang H, Freitas D, Kim HS, Fabijanic K, Li Z, Chen H, Mark MT, Molina H, Martin AB, Bojmar L *et al*: Identification of distinct nanoparticles and subsets of extracellular vesicles by asymmetric flow field-flow fractionation. *Nat Cell Biol* 2018, 20(3):332-343.
- 15. Gu Y, Zhou G, Zhang M, Lu G, Shen F, Qi B, Hua K, Ding J: Bioengineered extracellular vesicles presenting PD-L1 and Gal-9 to ameliorate new-onset primary ovarian insufficiency (POI). *Chemical Engineering Journal* 2025, 512:162635.
- 16. Zhou G, Gu Y, Zhang M, Ding J, Lu G, Hua K, Shen F: Identification of genetically engineered strategies to manipulate nano-platforms presenting immunotherapeutic ligands for alleviating primary ovarian insufficiency

- progression. Cell Commun Signal 2025, 23(1):246.
- 17. Gao X, Ran N, Dong X, Zuo B, Yang R, Zhou Q, Moulton HM, Seow Y, Yin H: Anchor peptide captures, targets, and loads exosomes of diverse origins for diagnostics and therapy. *Sci Transl Med* 2018, 10(444).
- 18. Alvarez-Erviti L, Seow Y, Yin H, Betts C, Lakhal S, Wood MJ: Delivery of siRNA to the mouse brain by systemic injection of targeted exosomes. *Nat Biotechnol* 2011, 29(4):341-345.
- 19. Han G, Zhang Y, Zhong L, Wang B, Qiu S, Song J, Lin C, Zou F, Wu J, Yu H et al: Generalizable anchor aptamer strategy for loading nucleic acid therapeutics on exosomes. *EMBO Mol Med* 2024, 16(4):1027-1045.
- 20. Saad N, Duroux-Richard I, Touitou I, Jeziorski E, Apparailly F: MicroRNAs in inflammasomopathies. *Immunol Lett* 2023, 256-257:48-54.
- 21. Schütte JP, Manke MC, Hemmen K, Münzer P, Schörg BF, Ramos GC, Pogoda M, Dicenta V, Hoffmann SHL, Pinnecker J et al: Platelet-Derived MicroRNAs Regulate Cardiac Remodeling After Myocardial Ischemia. Circ Res 2023, 132(7):e96-e113.
- 22. Zeng H, Zhou Y, Liu Z, Liu W: MiR-21-5p modulates LPS-induced acute injury in alveolar epithelial cells by targeting SLC16A10. *Sci Rep* 2024, 14(1):11160.
- 23. Xue J, Liu J, Xu B, Yu J, Zhang A, Qin L, Liu C, Yang Y: miR-21-5p inhibits inflammation injuries in LPS-treated H9c2 cells by regulating PDCD4. *Am J Transl Res* 2021, 13(10):11450-11460.
- 24. Weber B, Henrich D, Marzi I, Leppik L: Decrease of exosomal miR-21-5p and the increase of CD62p+ exosomes are associated with the development of sepsis in polytraumatized patients. *Mol Cell Probes* 2024, 74:101954.
- 25. Zhang Y, Huang H, Liu W, Liu S, Wang XY, Diao ZL, Zhang AH, Guo W, Han X, Dong X *et al*: Endothelial progenitor cells-derived exosomal microRNA-21-5p alleviates sepsis-induced acute kidney injury by inhibiting

- RUNX1 expression. Cell Death Dis 2021, 12(4):335.
- 26. Watson DC, Johnson S, Santos A, Yin M, Bayik D, Lathia JD, Dwidar M: Scalable Isolation and Purification of Extracellular Vesicles from Escherichia coli and Other Bacteria. J Vis Exp 2021(176).
- 27. Welsh JA, Goberdhan DCI, O'Driscoll L, Buzas EI, Blenkiron C, Bussolati B, Cai H, Di Vizio D, Driedonks TAP, Erdbrügger U *et al*: Minimal information for studies of extracellular vesicles (MISEV2023): From basic to advanced approaches. *J Extracell Vesicles* 2024, 13(2):e12404.
- 28. Welsh JA, Arkesteijn GJA, Bremer M, Cimorelli M, Dignat-George F, Giebel B, Görgens A, Hendrix A, Kuiper M, Lacroix R *et al*: A compendium of single extracellular vesicle flow cytometry. *J Extracell Vesicles* 2023, 12(2):e12299.
- 29. Welsh JA, Van Der Pol E, Arkesteijn GJA, Bremer M, Brisson A, Coumans F, Dignat-George F, Duggan E, Ghiran I, Giebel B *et al*: MIFlowCyt-EV: a framework for standardized reporting of extracellular vesicle flow cytometry experiments. *J Extracell Vesicles* 2020, 9(1):1713526.
- 30. Zhang L, Jiao G, Ren S, Zhang X, Li C, Wu W, Wang H, Liu H, Zhou H, Chen Y: Exosomes from bone marrow mesenchymal stem cells enhance fracture healing through the promotion of osteogenesis and angiogenesis in a rat model of nonunion. *Stem Cell Res Ther* 2020, 11(1):38.
- 31. Yu L, Sui B, Fan W, Lei L, Zhou L, Yang L, Diao Y, Zhang Y, Li Z, Liu J *et al*: Exosomes derived from osteogenic tumor activate osteoclast differentiation and concurrently inhibit osteogenesis by transferring COL1A1-targeting miRNA-92a-1-5p. *J Extracell Vesicles* 2021, 10(3):e12056.
- 32. Li B, Xia C, He W, Liu J, Duan R, Ji Z, Pan X, Zhou Y, Yu G, Wang L: The Thyroid Hormone Analog GC-1 Mitigates Acute Lung Injury by Inhibiting M1 Macrophage Polarization. *Adv Sci (Weinh)* 2024, 11(44):e2401931.
- 33. Zhou G, Zhou F, Gu Y, Zhang M, Zhang G, Shen F, Hua K, Ding J: Vaginal Microbial Environment Skews Macrophage Polarization and Contributes to

- Cervical Cancer Development. J Immunol Res 2022, 2022:3525735.
- 34. Théry C, Witwer KW, Aikawa E, Alcaraz MJ, Anderson JD, Andriantsitohaina R, Antoniou A, Arab T, Archer F, Atkin-Smith GK *et al*: Minimal information for studies of extracellular vesicles 2018 (MISEV2018): a position statement of the International Society for Extracellular Vesicles and update of the MISEV2014 guidelines. *J Extracell Vesicles* 2018, 7(1):1535750.
- 35. Witwer KW, Goberdhan DC, O'Driscoll L, Théry C, Welsh JA, Blenkiron C, Buzás EI, Di Vizio D, Erdbrügger U, Falcón-Pérez JM *et al*: Updating MISEV: Evolving the minimal requirements for studies of extracellular vesicles. *J Extracell Vesicles* 2021, 10(14):e12182.
- 36. Li Y, Tang X, Gu Y, Zhou G: Adipocyte-Derived Extracellular Vesicles: Small Vesicles with Big Impact. *Front Biosci (Landmark Ed)* 2023, 28(7):149.
- 37. Théry C, Amigorena S, Raposo G, Clayton A: Isolation and characterization of exosomes from cell culture supernatants and biological fluids. *Curr Protoc Cell Biol* 2006, Chapter 3:Unit 3.22.
- 38. Thirunavukkarasu M, Swaminathan S, Kemerley A, Pradeep SR, Lim ST, Accorsi D, Wilson R, Campbell J, Saad I, Yee SP *et al*: Role of Pellino-1 in Inflammation and Cardioprotection following Severe Sepsis: A Novel Mechanism in a Murine Severe Sepsis Model (†). *Cells* 2023, 12(11).
- 39. Cox MI, Voss H: Improving sepsis recognition and management. *Curr Probl Pediatr Adolesc Health Care* 2021, 51(4):101001.
- 40. Rello J, Valenzuela-Sánchez F, Ruiz-Rodriguez M, Moyano S: Sepsis: A Review of Advances in Management. *Adv Ther* 2017, 34(11):2393-2411.
- 41. Yang K, Fan M, Wang X, Xu J, Wang Y, Tu F, Gill PS, Ha T, Liu L, Williams DL *et al*: Lactate promotes macrophage HMGB1 lactylation, acetylation, and exosomal release in polymicrobial sepsis. *Cell Death Differ* 2022, 29(1):133-146.
- 42. Patoli D, Mignotte F, Deckert V, Dusuel A, Dumont A, Rieu A, Jalil A, Van

- Dongen K, Bourgeois T, Gautier T *et al*: Inhibition of mitophagy drives macrophage activation and antibacterial defense during sepsis. *J Clin Invest* 2020, 130(11):5858-5874.
- 43. Shapouri-Moghaddam A, Mohammadian S, Vazini H, Taghadosi M, Esmaeili SA, Mardani F, Seifi B, Mohammadi A, Afshari JT, Sahebkar AA-O: Macrophage plasticity, polarization, and function in health and disease. *J Cell Physiol* 2018, 233(9):6425-6440.
- 44. Atri CA-O, Guerfali FA-O, Laouini D: Role of Human Macrophage Polarization in Inflammation during Infectious Diseases. LID 10.3390/ijms19061801 [doi] LID 1801. *Int J Mol Sci* 2018, 19(6):1801.
- 45. Li ZA-O, Xiao JA-O, Xu XA-O, Li WA-O, Zhong RA-O, Qi LA-O, Chen J, Cui GA-O, Wang SA-O, Zheng YA-O *et al*: M-CSF, IL-6, and TGF-β promote generation of a new subset of tissue repair macrophage for traumatic brain injury recovery. LID 10.1126/sciadv.abb6260 [doi] LID eabb6260. *Sci Adv* 2021, 7(11):eabb6260.
- 46. Bouchareychas L, Duong P, Covarrubias S, Alsop E, Phu TA, Chung A, Gomes M, Wong D, Meechoovet B, Capili A *et al*: Macrophage Exosomes Resolve Atherosclerosis by Regulating Hematopoiesis and Inflammation via MicroRNA Cargo. *Cell Rep* 2020, 32(2):107881.
- 47. Pajarinen J, Lin T, Gibon E, Kohno Y, Maruyama M, Nathan K, Lu L, Yao Z, Goodman SB: Mesenchymal stem cell-macrophage crosstalk and bone healing. *Biomaterials* 2019, Mar(196):80-89.
- 48. Tobita M, Orbay H Fau Mizuno H, Mizuno H: Adipose-derived stem cells: current findings and future perspectives. *Discov Med* 2011, 11(57):160-170.
- 49. Payab M, Goodarzi P, Foroughi Heravani N, Hadavandkhani M, Zarei Z, Falahzadeh K, Larijani B, Rahim F, Arjmand B: Stem Cell and Obesity: Current State and Future Perspective. *Adv Exp Med Biol* 2018, 2018(1089):1-22.

- 50. Zheng G Fau Huang L, Huang L Fau Tong H, Tong H Fau Shu Q, Shu Q Fau Hu Y, Hu Y Fau Ge M, Ge M Fau Deng K, Deng K Fau Zhang L, Zhang L Fau Zou B, Zou B Fau Cheng B, Cheng B Fau Xu J et al: Treatment of acute respiratory distress syndrome with allogeneic adipose-derived mesenchymal stem cells: a randomized, placebo-controlled pilot study. Respir Res 2014, 15(1):39.
- 51. Sun J, Ding X, Liu S, Duan X, Liang H, Sun TA-O: Adipose-derived mesenchymal stem cells attenuate acute lung injury and improve the gut microbiota in septic rats. *Stem Cell Res Ther* 2020, 11(1):384.
- 52. van Niel G, D'Angelo G, Raposo G: Shedding light on the cell biology of extracellular vesicles. *Nat Rev Mol Cell Biol* 2018, 19(4):213-228.
- 53. Wang G, Li J, Bojmar L, Chen H, Li Z, Tobias GC, Hu M, Homan EA, Lucotti S, Zhao F et al: Tumour extracellular vesicles and particles induce liver metabolic dysfunction. *Nature* 2023, 618(7964):374-382.
- 54. Li Z, Low VA-OX, Luga V, Sun J, Earlie E, Parang B, Shobana Ganesh K, Cho S, Endress J, Schild T *et al*: Tumor-produced and aging-associated oncometabolite methylmalonic acid promotes cancer-associated fibroblast activation to drive metastatic progression. *Nat Commun* 2022, 13(1):6239.
- 55. Abels ER, Breakefield XO: Introduction to Extracellular Vesicles: Biogenesis, RNA Cargo Selection, Content, Release, and Uptake. *Cell Mol Neurobiol* 2016, 36(3):301-312.
- 56. Kenific CM, Zhang HA-O, Lyden D: An exosome pathway without an ESCRT. *Cell Res* 2021, 31(2):105-106.
- 57. Choi HA-O, Kim YA-OX, Mirzaaghasi AA-O, Heo JA-O, Kim YN, Shin JA-O, Kim SA-O, Kim NA-O, Cho EA-O, In Yook JA-O *et al*: Exosome-based delivery of super-repressor IκBα relieves sepsis-associated organ damage and mortality. *Sci Adv* 2020, 6(15):eaaz6980.
- 58. Qian W, Wu E, Chen H, Yao J, Wang J, Zhou Y, Bai Y, Wang S, Shen C, Li Y

- et al: MSCs-exosomes can promote macrophage M2 polarization via exosomal miR-21-5p through Mesenteric injection: a promising way to attenuate murine colitis. *J Crohns Colitis* 2024.
- 59. Hu Z, You L, Hu S, Yu L, Gao Y, Li L, Zhang S: Hepatocellular carcinoma cell-derived exosomal miR-21-5p promotes the polarization of tumor-related macrophages (TAMs) through SP1/XBP1 and affects the progression of hepatocellular carcinoma. *Int Immunopharmacol* 2024, 126:111149.
- 60. Agarwal V, Bell GW, Nam JW, Bartel DP: Predicting effective microRNA target sites in mammalian mRNAs. *Elife* 2015, 4.
- 61. Lu J, Getz G, Miska EA, Alvarez-Saavedra E, Lamb J, Peck D, Sweet-Cordero A, Ebert BL, Mak RH, Ferrando AA *et al*: MicroRNA expression profiles classify human cancers. *Nature* 2005, 435(7043):834-838.
- 62. Jain K, Mohan KV, Roy G, Sinha P, Jayaraman V, Kiran, Yadav AS, Phasalkar A, Deepanshu, Pokhrel A et al: Reconditioned monocytes are immunomodulatory and regulate inflammatory environment in sepsis. Sci Rep 2023, 13(1):14977.
- 63. Xie Z, Lin B, Jia X, Su T, Wei Y, Tang J, Yang C, Cui C, Liu J: Enhanced IL-10 inhibits proliferation and promotes apoptosis of HUVECs through STAT3 signaling pathway in sepsis. *Histol Histopathol* 2021, 36(11):1179-1187.
- 64. Fan L, Yao L, Li Z, Wan Z, Sun W, Qiu S, Zhang W, Xiao D, Song L, Yang G et al: Exosome-Based Mitochondrial Delivery of circRNA mSCAR Alleviates Sepsis by Orchestrating Macrophage Activation. *Adv Sci (Weinh)* 2023, 10(14):e2205692.
- 65. Chen X, Liu Y, Gao Y, Shou S, Chai Y: The roles of macrophage polarization in the host immune response to sepsis. *Int Immunopharmacol* 2021, 96:107791.
- 66. Kuang Y, Zheng X, Zhang L, Ai X, Venkataramani V, Kilic E, Hermann DM,

- Majid A, Bähr M, Doeppner TR: Adipose-derived mesenchymal stem cells reduce autophagy in stroke mice by extracellular vesicle transfer of miR-25. *J Extracell Vesicles* 2020, 10(1):e12024.
- 67. Hwang S, Park J, Koo SY, Lee SY, Jo Y, Ryu D, Go H, Lee CW: The ubiquitin ligase Pellino1 targets STAT3 to regulate macrophage-mediated inflammation and tumor development. *Nat Commun* 2025, 16(1):1256.
- 68. Dai D, Zhou H, Yin L, Ye F, Yuan X, You T, Zhao X, Long W, Wang D, He X et al: PELI1 promotes radiotherapy sensitivity by inhibiting noncanonical NF-κB in esophageal squamous cancer. Mol Oncol 2022, 16(6):1384-1401.
- 69. Silva AM, Lázaro-Ibáñez E, Gunnarsson A, Dhande A, Daaboul G, Peacock B, Osteikoetxea X, Salmond N, Friis KP, Shatnyeva O *et al*: Quantification of protein cargo loading into engineered extracellular vesicles at single-vesicle and single-molecule resolution. *J Extracell Vesicles* 2021, 10(10):e12130.

TABLES AND FIGURES WITH LEGENDS

Table 1. qRT-PCR primers used for human and mouse genes

Gene name sequence (5'-3')	qRT-PCR primers:
CD163 (human)	F: TTTGTCAACTTGAGTCCCTTCAC
	R: TCCCGCTACACTTGTTTTCAC
CD163 (mouse)	F: TTTGTCAACTTGAGTCCCTTCAC
	R: TCCCGCTACACTTGTTTTCAC
IL10 (human)	F: GACTTTAAGGGTTACCTGGGTTG
	R: TCACATGCGCCTTGATGTCTG
IL10 (mouse)	F: GACTTTAAGGGTTACCTGGGTTG
	R: TCACATGCGCCTTGATGTCTG
ARG1 (human)	F: TTGGGTGGATGCTCACACTG
	R: GTACACGATGTCTTTGGCAGA
Arg-1 (mouse)	F: TTGGGTGGATGCTCACACTG
	R: GTACACGATGTCTTTGGCAGA
GAPDH (human)	F:
	CGGAGTCAACGGATTTGGTCGTAT
	R:
	AGCCTTCTCCATGGTGGTGAAGAC
Gapdh (mouse)	F:
	CGGAGTCAACGGATTTGGTCGTAT
	R:
	AGCCTTCTCCATGGTGGTGAAGAC
miR21-5p (human)	F: CCCCCTAGCTTATCAGACTGATG
	R: CCAGTGCAGGGTCCGAGGT
miR21-5p (mouse)	F: CCCCCTAGCTTATCAGACTGATG
	R: CCAGTGCAGGGTCCGAGGT

	R:
	GCTTCGGCAGCACATATACTAAAAT
U6 (mouse)	F: CGCTTCACGAATTTGCGTGTCAT
	R:
	GCTTCGGCAGCACATATACTAAAAT
CD68 (human)	F: AGGAGACACAGGAAATGGAG
	R: ATGGATGCTGGAGTGATGAA
CD68 (mouse)	F: CCGGAAGAAAGGAGATAGGAG
	R: CCTGAGGACTCCTTCCATG
IL6 (human)	F: GAAAGCAGCCAGAGTCATTC
	R: CAAGGAGAGACTTGCAGAGA
IL6 (mouse)	F:
	CAAAGGAGGAGACTTGCAGAGA
	R: CAAGGAGAGACTTGCAGAGA

Abbreviations: Arg-1: Arginase 1; GAPDH: Glyceraldehyde-3-phosphate

dehydrogenase; F: Forward primer; R: Reverse primer.

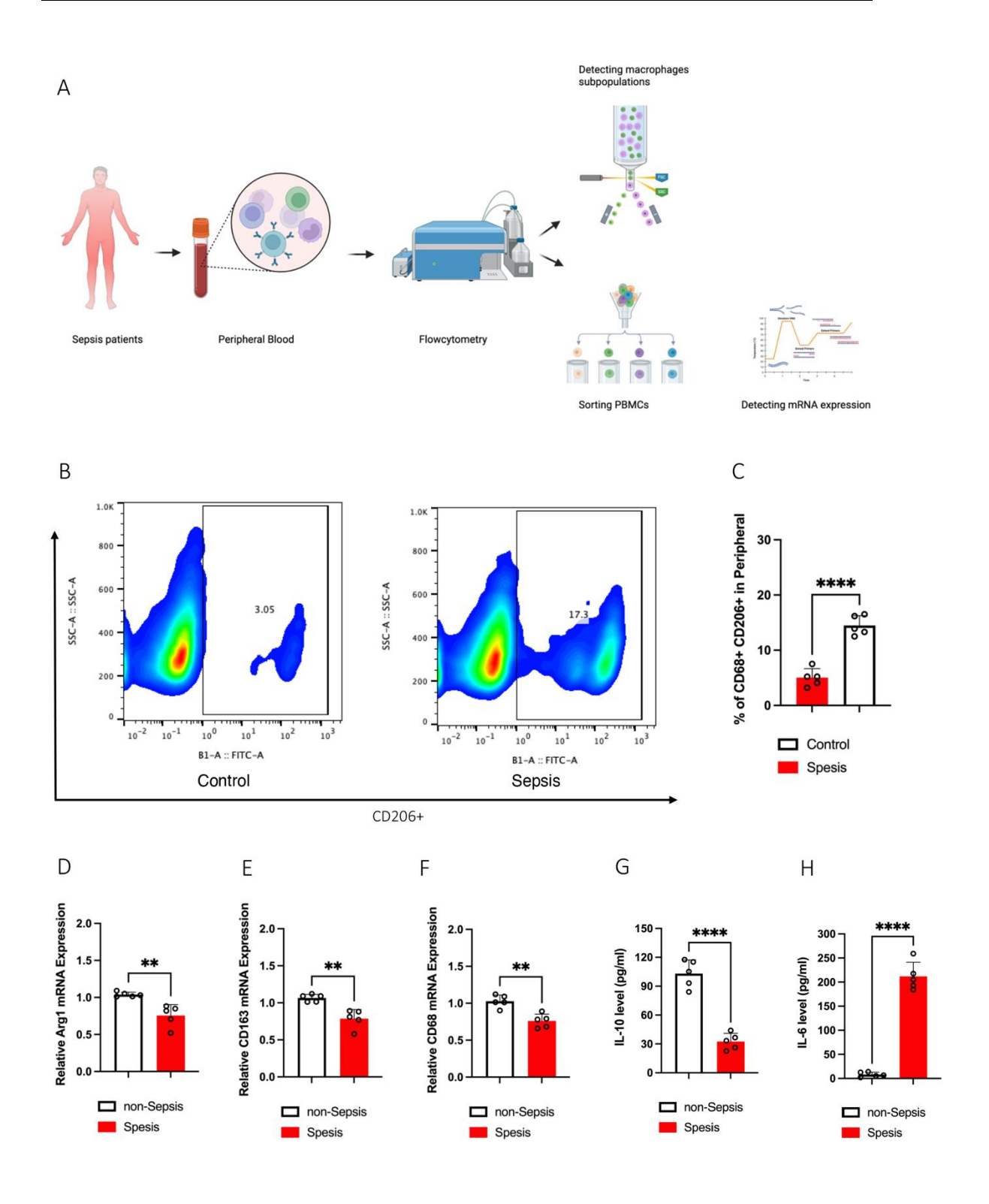


Figure 1. Macrophage phenotype subpopulations in serum with and without

sepsis. (A) Flowchart for the detection of macrophage phenotype subpopulations in serum from patients with and without sepsis. (B) Representative image showing the percentage of CD68+CD206+ cells in serum from patients with and without sepsis, as

determined by flow cytometry. (C) Quantitative analysis of the percentage of CD68+CD206+ cells in serum from patients with sepsis (n=10) compared to those without sepsis (n=10). (D) mRNA expression levels of Arg1 in PBMCs from patients with sepsis (n=10) versus those without sepsis (n=10). (E) mRNA expression levels of CD163 in PBMCs from patients with sepsis (n=10) and without sepsis (n=10). (F) mRNA expression levels of CD68 in PBMCs from patients with sepsis (n=10) and without sepsis (n=10). (G) Cytokine expression levels of IL-10 in serum from septic patients (n=10) compared to non-septic patients (n=10). (H) Cytokine expression levels of IL-6 in serum from septic patients (n=10) versus non-septic patients (n=10). Abbreviations: Arg1: Arginase 1; PBMCs: Peripheral blood mononuclear cells.

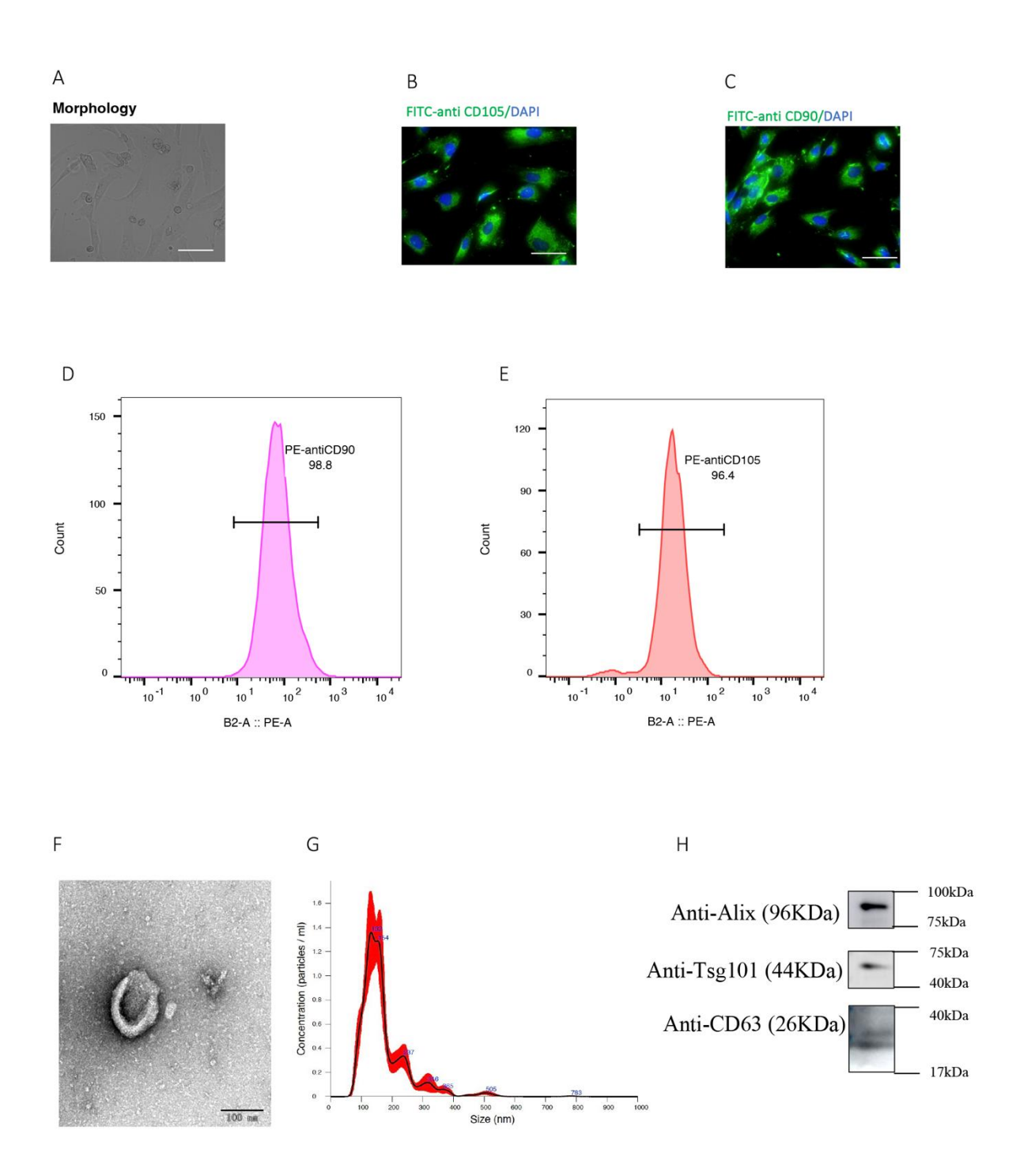


Figure 2. Isolation and identification of ADMSCs and ADMSC-EVs. (A) The morphological characteristics of primary ADMSCs were examined using a microscope. (B) The surface marker CD105 of ADMSCs was detected using fluorescence microscopy. (C) The surface marker CD90 of ADMSCs was also

detected via fluorescence microscopy. (D) The expression of CD105 in ADMSCs is shown, with blue indicating the isotype control and red indicating CD90 positivity. (E) The expression of CD90 in ADMSCs is depicted, with red representing the isotype control and blue indicating CD90 positivity. (F) The size distribution of ADMSC-EVs was analyzed using NTA. (G) The surface markers (CD63, Alix, and Tsg101) of ADMSC-EVs were evaluated by western blot analysis. (H) The morphological characteristics of ADMSC-EVs were observed using a transmission electron microscope. Abbreviations: ADMSCs: Adipose-derived mesenchymal stem cells; ADMSC-EVs: Adipose-derived mesenchymal stem cell—derived extracellular vesicles; NTA: Nanoparticle tracking analysis; Alix: ALG-2-interacting protein X.

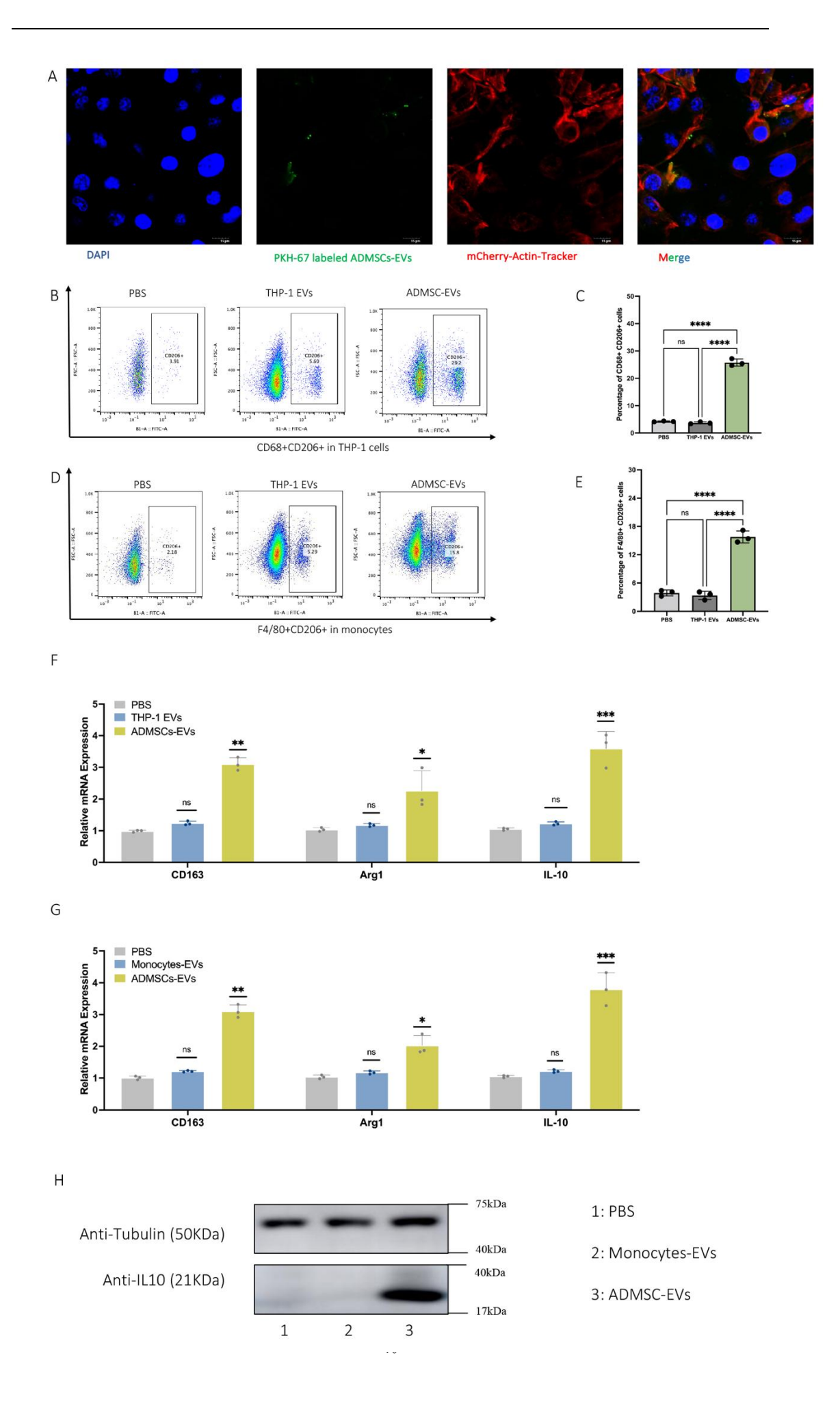


Figure 3. ADMSC-EVs induce macrophages polarization into M2 phenotype in vitro and ex vivo. (A) Uptake of ADMSC-EVs by THP-1 cells, as indicated by PKH-67 labeling and mCherry-Actin Tracker. (B) THP-1 cells treated with ADMSC-EVs exhibited a significantly higher percentage of CD68+CD206+ cells compared to those treated with PBS or THP-1 EVs. (C) Quantitative analysis of the percentage of CD68+CD206+ cells following various treatments. (D) Primary monocytes treated with ADMSC-EVs showed an increased percentage of CD68+CD206+ cells compared to those treated with PBS or THP-1 EVs. (E) Quantitative analysis of the percentage of CD68+CD206+ cells after different treatments. (F) mRNA expression levels of CD163, Arg1, and IL-10 in THP-1 cells treated with PBS, THP-1 EVs, and ADMSC-EVs. (G) mRNA expression levels of CD163, Arg1, and IL-10 in primary monocytes treated with PBS, THP-1 EVs, and ADMSC-EVs. (H) Protein expression levels of IL-10 in primary monocytes treated with PBS, Monocyte-EVs, and ADMSC-EVs. Abbreviations: ADMSC-EVs: Adipose-derived mesenchymal stem cell–derived extracellular vesicles; PKH-67: Lipophilic fluorescent membrane dye; PBS: Phosphate-buffered saline; EVs: Extracellular vesicles; Arg1: Arginase 1.

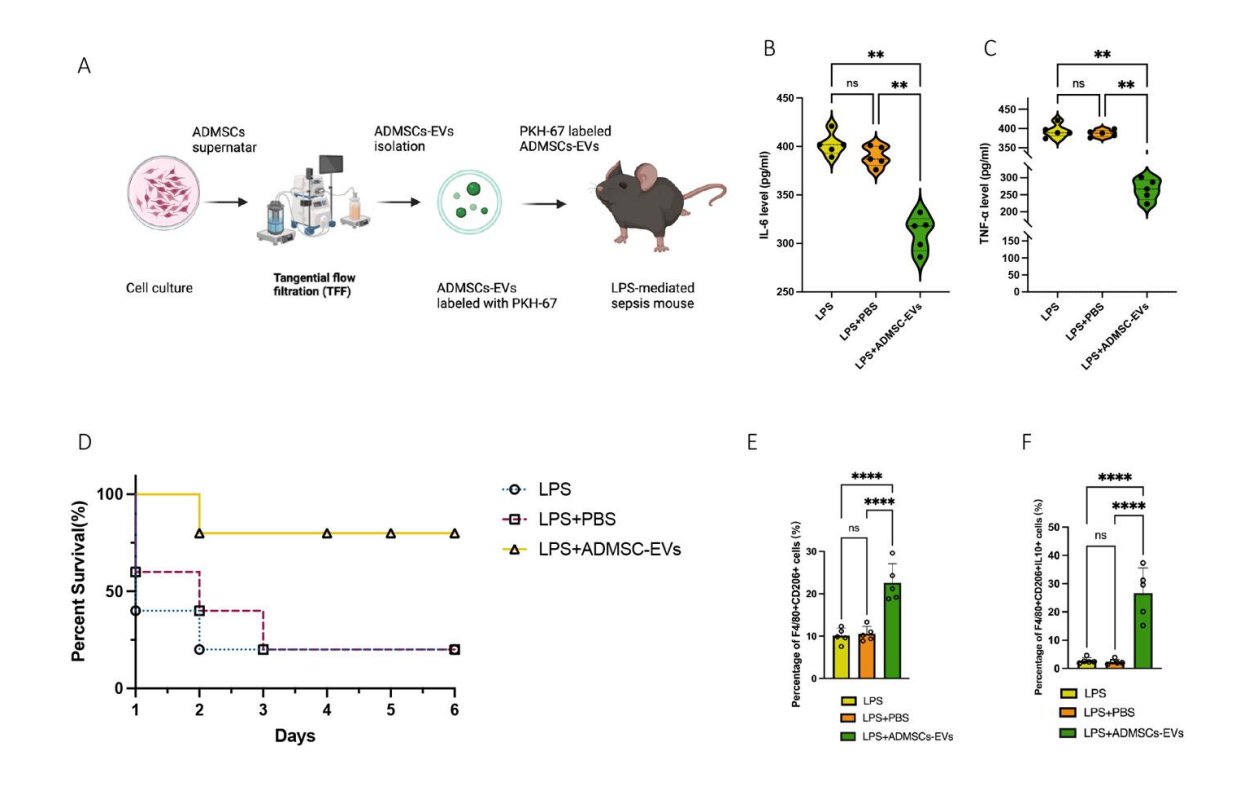


Figure 4. ADMSC-EVs alleviate LPS-induced sepsis. (A) Flowchart illustrating the isolation and injection of ADMSC-EVs into LPS-induced septic mice. (B) The expression levels of IL-6 in LPS-mediated septic mice, treated with no intervention, PBS, or ADMSC-EVs, were measured using ELISA. (C) The expression levels of TNF-α in LPS-mediated septic mice, treated with no intervention, PBS, or ADMSC-EVs, were assessed via ELISA. (D) The survival rates of mice over a 6-day period (LPS group: *n*= 5; LPS + PBS group: *n*= 5; LPS + ADMSC-EVs group: *n*= 5). (E) The percentage of F4/80+ CD206+ cells among PBMCs was analyzed following treatment with ADMSC-EVs, PBS, or no treatment for 12 hours via flow cytometry. (F) The percentage of F4/80+ CD206+ IL-10+ cells among PBMCs was evaluated after treatment with ADMSC-EVs, PBS, or no treatment for 12 hours via flow cytometry. Abbreviations: ADMSC-EVs: Adipose-derived mesenchymal stem cell–derived extracellular vesicles; LPS: Lipopolysaccharide; TNF-α: Tumor necrosis factor alpha; PBMCs: Peripheral blood mononuclear cells; PBS: Phosphate-buffered saline.

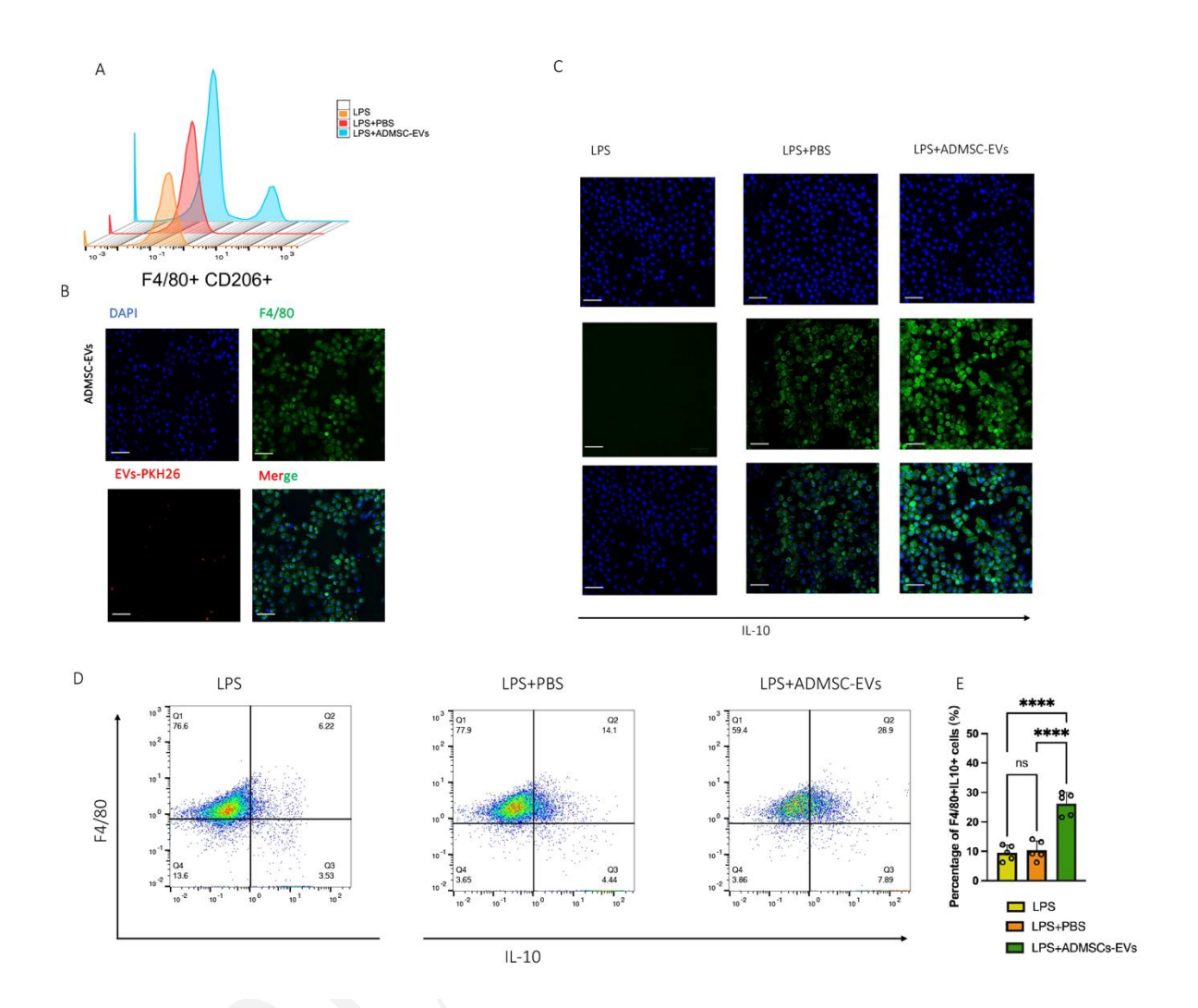


Figure 5. ADMSC-EVs induce the IL-10 secretion in macrophage *in vivo*. (A) PKH-67-labeled ADMSC-EVs were encapsulated within F4/80-positive macrophages. The co-localization of EVs (PKH67-labeled green) and macrophages (F4/80, red) in lung tissue was assessed using immunofluorescence staining. (B) The percentage of F4/80+ CD206+ macrophages in lung tissue from mice was measured following ADMSC-EV treatment. (C) The expression of IL-10 in lung tissue was evaluated via immunofluorescence staining. (D) The expression of IL-10 in F4/80+ lung macrophages from sepsis mice treated with ADMSC-EVs was determined. Abbreviations: ADMSC-EVs: Adipose-derived mesenchymal stem cell-derived extracellular vesicles; PKH-67: Lipophilic fluorescent membrane dye; EVs: Extracellular vesicles.

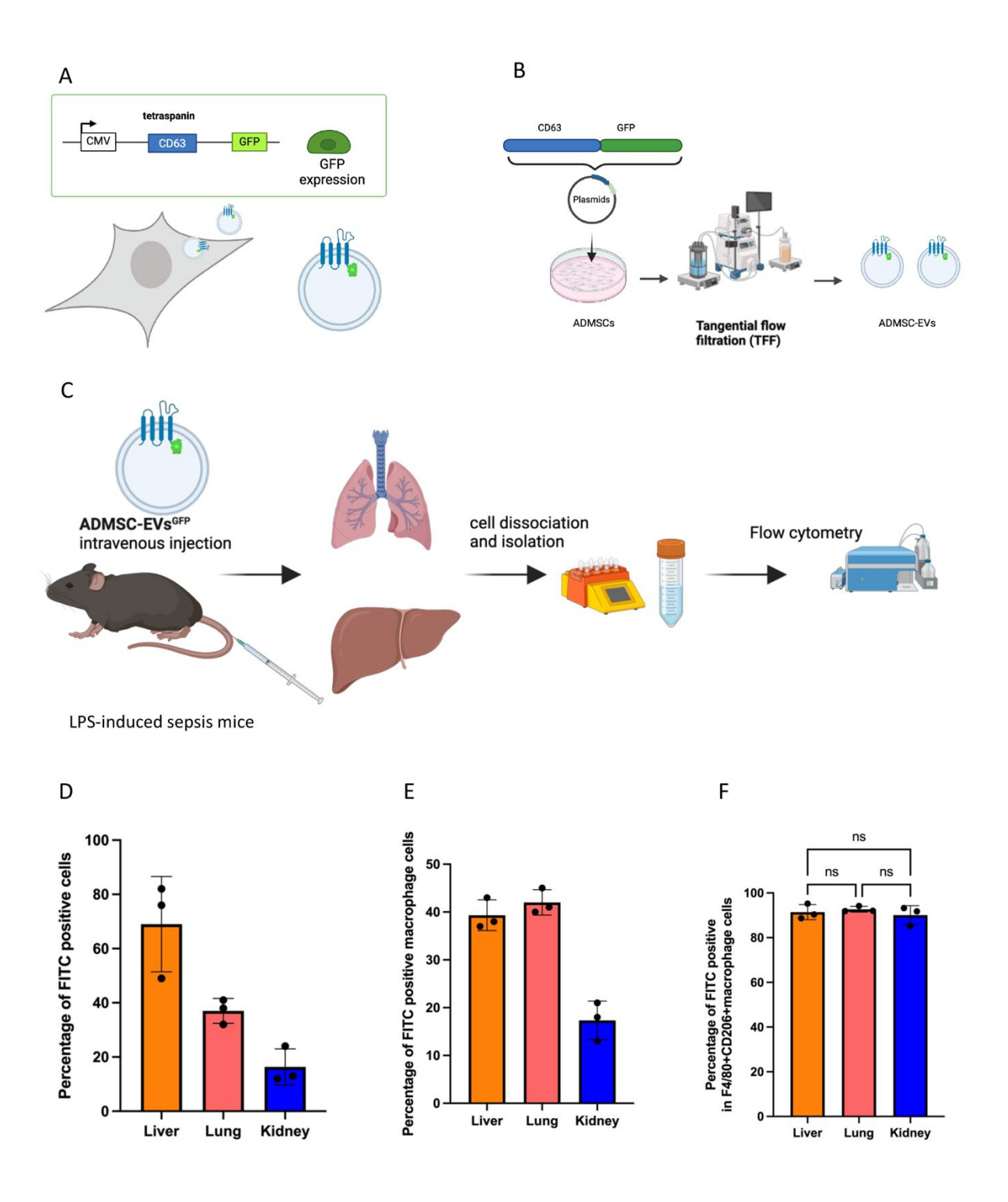


Figure 6. *In vivo* biodistribution of ADMSC-EVs. (A) Flowchart of plasmid "Plex-CD63-GFP" for engineered ADMSC-EVsGFP. (B) Flowchart of biogenesis process for producing ADMSC-EVsGFP. (C) Flowchart detailing the experimental setup for administering ADMSC-EVsGFP to septic mice to assess their

biodistribution *in vivo*. (D) Flow cytometric analysis revealing the percentage of FITC+ cells in the liver, lung, and kidney of septic mice. (E) Flow cytometric analysis indicating the percentage of FITC+ macrophages in the liver, lung, and kidney of septic mice. (F) Flow cytometric analysis showing the percentage of FITC+ M2 macrophages in the liver, lung, and kidney of septic mice. Abbreviations:

ADMSC-EVsGFP: Green fluorescent protein—labeled adipose-derived mesenchymal stem cell—derived extracellular vesicles; GFP: Green fluorescent protein; FITC: Fluorescein isothiocyanate.

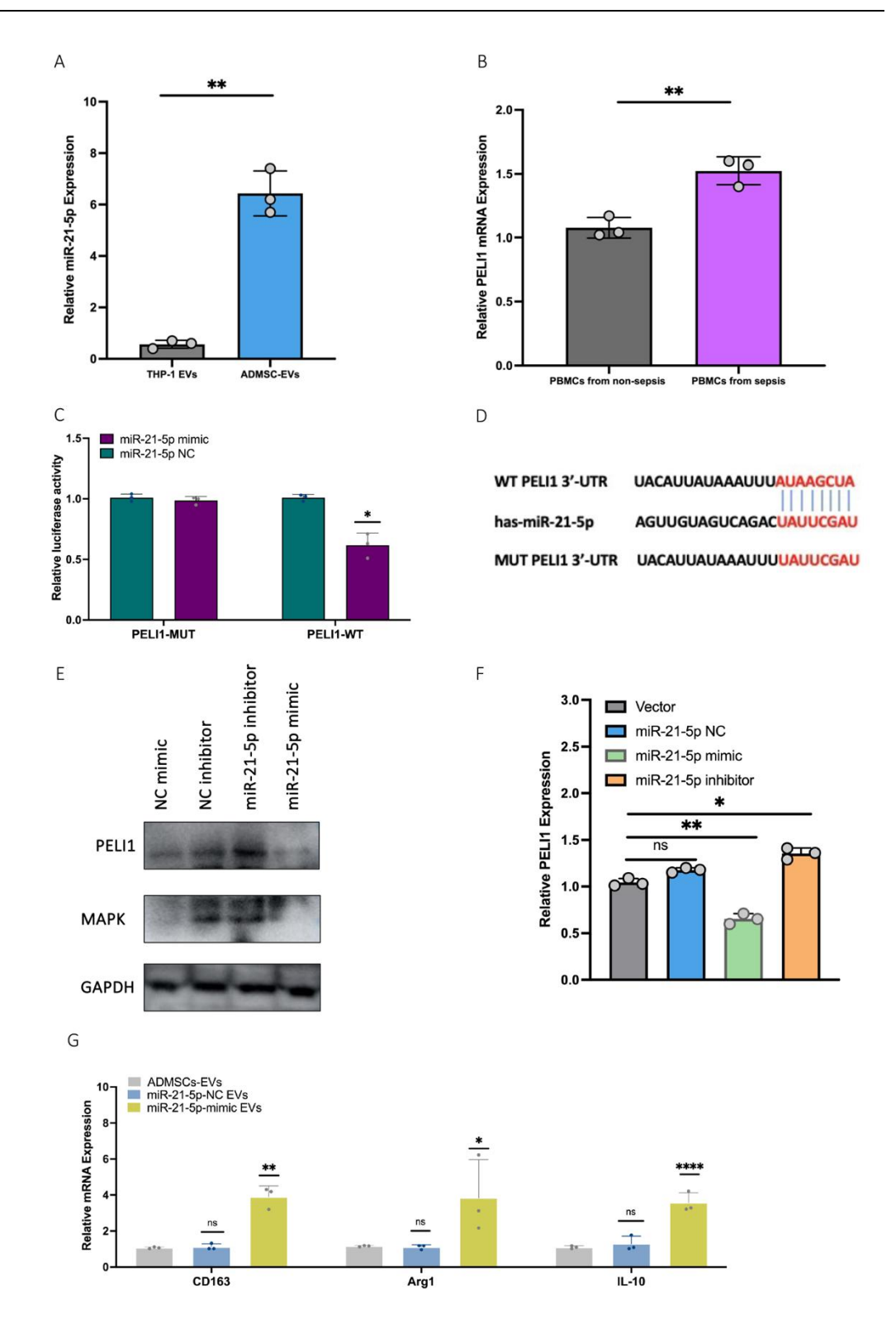


Figure 7. ADMSC-EVs encapsulated miR-21-5p targeting *PELI1* in macrophages. (A) Expression levels of miR-21-5p in THP-1 EVs and ADMSC-EVs. (B) mRNA expression levels of *PELI1* in PBMCs from sepsis and non-sepsis patients. (C) Evaluation of the interaction between miR-21-5p and *PELI1* using a

dual-luciferase reporter assay. (D) Analysis of the binding site of has-miR-21-5p (the mature form of human miR-21 derived from the 5' arm of its precursor hairpin structure) and *PELI1* using TargetScan software. (E) Protein expression levels of PELI1 following regulation of miR-21-5p expression. (F) mRNA expression levels of *PELI1* after regulation of miR-21-5p expression. (G) mRNA expression levels of *CD163*, *Arg1*, and *IL-10* following regulation of miR-21-5p expression.

Abbreviations: ADMSC-EVs: Adipose-derived mesenchymal stem cell–derived extracellular vesicles; EVs: Extracellular vesicles; PBMCs: Peripheral blood mononuclear cells; *PELI1*: Pellino E3 ubiquitin protein ligase 1; *Arg1*: Arginase 1.

SUPPLEMENTAL DATA

Supplemental data are available at the following link:

https://www.bjbms.org/ojs/index.php/bjbms/article/view/11971/4030